

**Neutron-proton multiplets in the nucleus  $^{88}\text{Br}$** 

M. Czerwiński,<sup>1</sup> T. Rząca-Urban,<sup>1</sup> W. Urban,<sup>1</sup> P. Bączyk,<sup>1</sup> K. Sieja,<sup>2,3</sup> B. M. Nyakó,<sup>4</sup> J. Timár,<sup>4</sup> I. Kuti,<sup>4</sup> T. G. Tornyi,<sup>4</sup> L. Atanasova,<sup>5</sup> A. Blanc,<sup>6</sup> M. Jentschel,<sup>6</sup> P. Mutti,<sup>6</sup> U. Köster,<sup>6</sup> T. Soldner,<sup>6</sup> G. de France,<sup>7</sup> G. S. Simpson,<sup>8,9</sup> and C. A. Ur

<sup>1</sup>*Faculty of Physics, University of Warsaw, ul. Pasteura 5, PL-02-093 Warsaw, Poland*

<sup>2</sup>*Université de Strasbourg, IPHC, Strasbourg, France*

<sup>3</sup>*CNRS, UMR7178, 67037 Strasbourg, France*

<sup>4</sup>*Institute for Nuclear Research, Hungarian Academy of Sciences, Pf. 51, 4001 Debrecen, Hungary*

<sup>5</sup>*Department of Medical Physics and Biophysics, Medical University - Sofia, 1431, Sofia, Bulgaria*

<sup>6</sup>*Institut Laue-Langevin, Grenoble, France*

<sup>7</sup>*Grand Accélérateur National d'Ions Lourds (GANIL), CEA/DSM - CNRS/IN2P3, Boulevard Henri Becquerel, BP 55027, F-14076 Caen Cedex 5, France*

<sup>8</sup>*LPSC, Université Joseph Fourier Grenoble 1, CNRS/IN2P3, Institut National Polytechnique de Grenoble, F-38026 Grenoble Cedex, France*

<sup>9</sup>*University of the West of Scotland, Paisley, PA1 2BE, United Kingdom*

<sup>10</sup>*INFN, Legnaro, Italy*

(Received 31 March 2015; revised manuscript received 25 May 2015; published 30 July 2015)

Medium spin excited levels in  $^{88}\text{Br}$  populated in fission of  $^{235}\text{U}$  induced by neutrons have been observed for the first time. The measurement of  $\gamma$  radiation following fission has been performed using the EXILL array of Ge detectors at the cold-neutron beam facility PF1B of the Institut Laue-Langevin (ILL), Grenoble. The ground state of  $^{88}\text{Br}$  is proposed to be  $1^-$ , changing the adopted ( $2^-$ ) value. The low-energy, newly observed levels are members of the  $\pi p_{3/2} \nu(d_{5/2})^3$  and  $\pi f_{5/2}^{-1} \nu(d_{5/2})^3$  multiplets. A triplet of yrast levels observed at around 2 MeV is interpreted as being due to coupling of the  $g_{9/2}$  proton to the  $(d_{5/2})^3$ , seniority 3 multiplet, supporting the presence of collective effects in  $^{88}\text{Br}$ . The position of the  $g_{9/2}$  proton intruder in the  $^{78}\text{Ni}$  core is determined at 5.7 MeV above the  $f_{5/2}$  proton level. Shell-model calculations predict the same proton-neutron excitations proposed in  $^{88}\text{Br}$ .

DOI: [10.1103/PhysRevC.92.014328](https://doi.org/10.1103/PhysRevC.92.014328)

PACS number(s): 23.20.Lv, 23.20.Gq, 25.85.-w, 27.50.+e

**I. INTRODUCTION**

Properties of the  $^{78}\text{Ni}$  nucleus and its neighbors are expected to influence the path of the astrophysical  $r$  process. It is of interest to know whether and to what extent the  $Z = 28$  shell is still closed in nuclei past the  $N = 50$  neutron line and if any collectivity appears in this region. Extra collective correlations increase nuclear binding. This, in turn, may shift the  $r$ -process path, expected at around 2 MeV of neutron binding energy [1,2].

In our recent study [3] we have found clear signs of collectivity building up in the  $N = 53$  isotones below  $Z = 36$ , resulting in the so-called  $j$ -1 anomaly in the  $(d_{5/2})^3$  neutron multiplet, which produces the  $3/2^+$  ground states in  $^{89}\text{Kr}$  and  $^{87}\text{Se}$ . State-of-the-art shell-model calculations [4] have reproduced well collective effects at  $N = 53$  [3] and predicted collective excitations also in the  $^{86}\text{Se}$  nucleus at  $N = 52$  [5,6]. Both the experimental trend in the  $N = 53$  isotones and the shell-model predictions suggested a similar  $\nu(d_{5/2})_{j-1,j}^3$  doublet also in the  $^{85}\text{Ge}$  isotone. Such a doublet in  $^{85}\text{Ge}$  has been observed experimentally [7].

It is interesting to see if this trend continues towards lower  $Z$ . As the experimental verification of this effect at  $Z = 30$  is still not available, it is of interest to use the shell model to study these exotic nuclei. We have successfully used the shell model to describe properties of Se, Kr [3,5], Rb [8,9], and Sr [10] isotopes. It is also of interest to check whether one can use this description for Br isotopes. For this reason we have undertaken a systematic study of bromine isotopes.

In this work we report on the study of yrast excited levels in  $^{88}\text{Br}$  populated in fission of  $^{235}\text{U}$  induced by cold neutrons. The proton-neutron multiplets in  $^{88}\text{Br}$ , the odd-odd neighbor of  $^{87}\text{Se}$ , should provide a particularly useful testing ground for the shell-model ingredients in this region. In the work we report, for the first time, medium-spin excitations in  $^{88}\text{Br}$ , interpret them in terms of proton-neutron configurations, and use this data to test the shell-model predictions. The experiment is described in Sec. II A and the experimental results in Sec. II B. This is followed by the interpretation of the data (Sec. III). The work is concluded in Sec. IV.

**II. EXPERIMENT AND RESULTS****A. Experimental details**

We have searched for excited levels in  $^{88}\text{Br}$  using the EXILL spectrometer [11] at the PF1B cold-neutron beam [12] of the Institut Laue-Langevin in Grenoble. The array included eight Compton-suppressed EXOGAM Clover detectors [13], six Compton-suppressed GASP detectors [14] and two Clover detectors of the Lohengrin spectrometer [15]. The distance between faces of the detectors and target was about 15 cm. The collimation system described in [16] was installed at the PF1B to create a pencil neutron beam of about 12 mm diameter and a thermal equivalence flux of  $1 \times 10^8 / (\text{s cm}^2)$ . Neutron-rich nuclei were produced by cold-neutron-induced fission of 0.6 mg of  $^{235}\text{U}$ . The data were collected in a triggerless mode using a digital acquisition system with a 100 MHz clock [17],

which has delivered 15 terabytes of data over a period of 21 days. During the offline analysis triggerless events, each consisting of an energy signal and the time of its registration, were arranged into coincidence events within various time windows (from 200 to 2400 ns) and sorted into 2D and 3D histograms, which were then used to search for new  $\gamma$  decays in  $^{88}\text{Br}$ .

### B. Excitation scheme of $^{88}\text{Br}$

No medium-spin levels were reported in the odd-odd  $^{88}\text{Br}$  nucleus prior to this work. In Ref. [18], Zendel *et al.* reported several excited levels with low spins, populated in  $\beta^-$  decay of the  $0^+$  ground state of  $^{88}\text{Se}$ . They suggested spin and parity  $I^\pi = (1, 2^-)$  for the ground state of  $^{88}\text{Br}$ . Later, Genevey *et al.* reported a cascade of two delayed 110.9- and 159.1-keV transitions from the 5.1  $\mu\text{s}$  isomer at 270.0 keV [19]. The internal conversion coefficients for the 110.9- and 159.1-keV transitions show that the isomer decays by an  $E2-M1$  cascade [19] and the authors proposed spin and parity  $I^\pi = (4^-)$  for the isomer,  $I^\pi = (2^-)$  for the 159.1-keV level, and  $I^\pi = (1^-)$  for the ground state. They also stated that the 270.0-keV isomer is a different level than the 272.7-keV level reported in Ref. [18], decaying to the 159.-keV level via the 113.5-keV transition.

In the cold-neutron-induced fission of  $^{235}\text{U}$ , on average 2.4 neutrons and no protons are emitted from the primary fission fragments, leading to the secondary fission fragments, which then deexcite by emitting  $\gamma$  rays. This means that  $\gamma$  rays from both complementary fragments are in prompt time coincidence, which allows one to search for unknown transitions in a given nucleus if the decay scheme of the fission partner is known. In fission of  $^{235}\text{U}$ , the most abundant complementary fragments to  $^{88}\text{Br}$  are  $^{145}\text{La}$  and  $^{146}\text{La}$ , accompanied by the emission of three and two neutrons, respectively ( $3n$  and  $2n$  channels). In order to find new transitions in  $^{88}\text{Br}$ , we have analyzed spectra doubly gated on strong transitions in  $^{145}\text{La}$  and  $^{146}\text{La}$ . In the analysis we have used triple- $\gamma$  histogram sorted with a 200 ns time window (prompt- $\gamma$  coincidences).

Figure 1 shows a  $\gamma$  spectrum doubly gated on the 172.0-keV and 366.2-keV lines of  $^{145}\text{La}$  [20]. Apart from known lines of  $^{145}\text{La}$  there are the 113.9- and 159.1-keV lines assigned

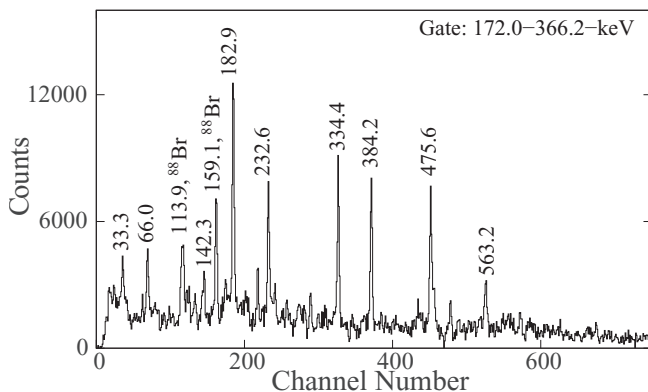


FIG. 1. A  $\gamma$ -ray spectrum doubly gated on the 172.0-keV and 366.2-keV  $\gamma$  lines of  $^{145}\text{La}$ . Energies of  $\gamma$  lines are labeled in keV.

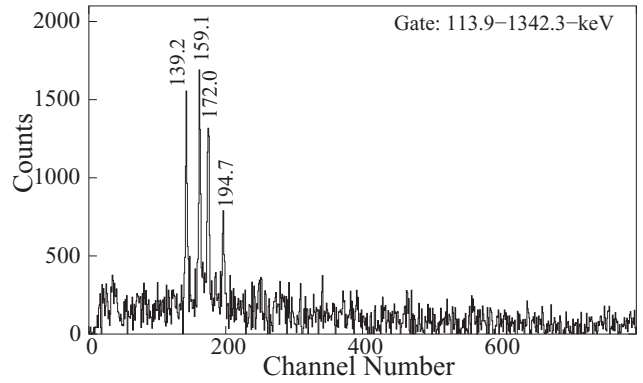


FIG. 2. A  $\gamma$ -ray spectrum doubly gated on the 113.9-keV and 1342.3-keV lines in  $^{88}\text{Br}$ .

previously to  $^{88}\text{Br}$  [18,19]. Their prompt coincidence with  $\gamma$  lines of  $^{145}\text{La}$  indicates that medium-spin levels of  $^{88}\text{Br}$  are populated in the fission of  $^{236}\text{U}$ .

Next, we have analyzed spectra doubly gated on one line of  $^{145}\text{La}$  or  $^{146}\text{La}$  and one of the 113.9- or 159.1-keV lines of  $^{88}\text{Br}$ . A new, pronounced line at 1342.3 keV have been observed and assigned to  $^{88}\text{Br}$ , based on coincidences with both  $^{145}\text{La}$  and  $^{146}\text{La}$ . In Fig. 2 we show a spectrum gated on the 113.9- and 1342.3-keV lines. In the spectrum four lines are clearly seen at 139.2, 159.1, 172.0, and 194.7 keV. The 172.0-keV transition belongs also to  $^{145}\text{La}$ . However, further double gating on the 172-keV line and the 130.4-keV line of  $^{146}\text{La}$  proves that the 172-keV line belongs also to  $^{88}\text{Br}$ .

Subsequent gates revealed an intense cascade of six transitions, 113.9, 139.2, 159.1, 172.0, 194.7, and 1342.3 keV, which belongs to the decay scheme of  $^{88}\text{Br}$ . In the  $\gamma$  spectrum doubly gated on the 139.2- and 159.1-keV lines, shown in Fig. 3, lines from this cascade and new lines at 126.6, 285.6, 406.2, 491.8, 604.8, 686.4, and 898.0 keV are seen. In Fig. 3 there is also x-ray line of the complementary lanthanum isotopes.

The above coincidence relations and further gates allowed the construction of the decay scheme of  $^{88}\text{Br}$  as shown in Fig. 4. Except for the 159.1-, 111.0-, 113.9-, and 259.5-keV transitions reported before [18,19], all other transitions are

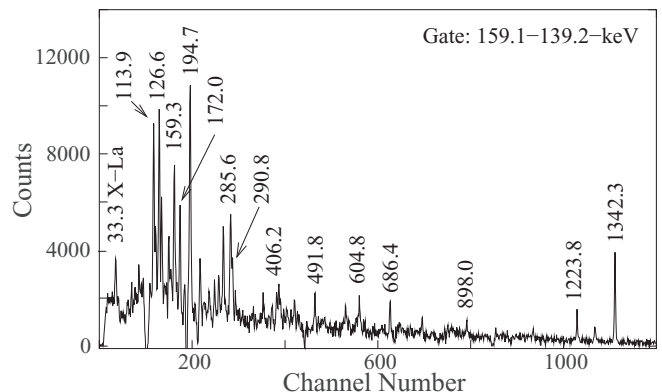


FIG. 3. A  $\gamma$ -ray spectrum doubly gated on the 159.1- and 139.2-keV lines in  $^{88}\text{Br}$ .

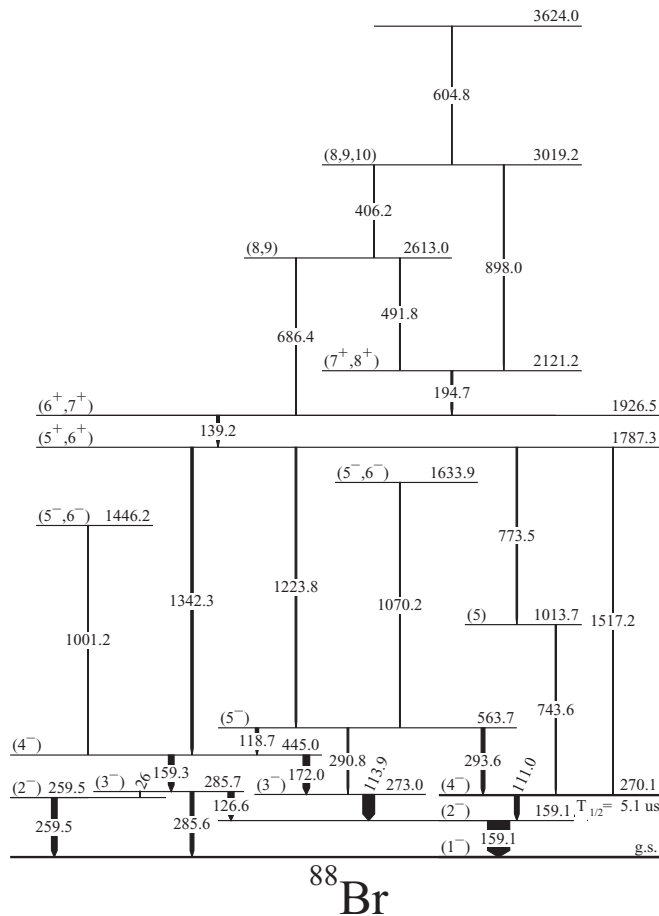


FIG. 4. Level scheme of  $^{88}\text{Br}$ , as obtained in the present work. The half-life of the 270.1-keV isomer is taken from Ref. [19]. The relative  $\gamma$ -ray intensities are listed in Table I.

new. The half-life of the 270.1-keV isomer is shown after Ref. [19].

The properties of transitions in  $^{88}\text{Br}$  observed in this work are presented in Table I. Spin and parity assignments to new levels in  $^{88}\text{Br}$  are discussed in Sec. II D. Below we comment

TABLE I. Properties of  $\gamma$  transitions in  $^{88}\text{Br}$ , as observed in the present work in neutron-induced fission of  $^{235}\text{U}$ .  $I_\gamma$  values are in arbitrary, relative units and correspond to prompt decays only (see text for comments on intensities of the 26.3- and 111.0-keV transitions).

$E_\gamma$ (keV)	$I_\gamma$ (rel.)	$E_\gamma$ (keV)	$I_\gamma$ (rel.)	$E_\gamma$ (keV)	$I_\gamma$ (rel.)
26.3		194.7(1)	16(2)	686.1(2)	6(1)
111.0(1)		259.5(2)	34(4)	743.6(2)	10(2)
113.9(1)	100(8)	285.6(2)	33(3)	773.5(2)	8(2)
118.7(1)	25(5)	290.8(2)	14(10)	898.0(2)	9(2)
126.6(1)	52(7)	293.6(1)	32(3)	1001.2(3)	3(1)
139.2(1)	23(3)	406.2(1)	2(1)	1070.2(2)	5(1)
159.1(1)	188(26)	480.0(3)	1(1)	1223.8(2)	13(3)
159.3(1)	48(8)	491.8(1)	6(1)	1342.3(1)	20(3)
172.0(1)	53(6)	604.8(2)	1(1)	1517.2(1)	6(1)

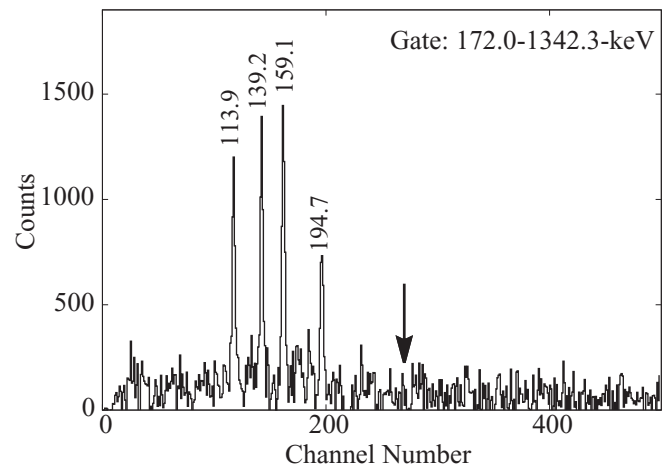


FIG. 5. A  $\gamma$ -ray spectrum doubly gated on the 172.0- and 1342.3-keV transitions in  $^{88}\text{Br}$ . Energies of  $\gamma$  lines are labeled in keV. The arrow marks the position of the 273.0-keV absent line.

on differences from previous works and show some specific evidence supporting the proposed decay scheme.

In Ref. [18] a direct decay from the 272.7-keV level to the ground state is reported, which is four times more intense than the 113.9-keV decay branch of this level. We do not confirm the presence of any 273-keV transition in  $^{88}\text{Br}$ . In Fig. 5 a  $\gamma$  spectrum doubly gated on the 172- and the 1342.3-keV lines is shown, which clearly shows the 113.9-, 139.2-, 159.1-, and 194.7-keV lines assigned to the  $^{88}\text{Br}$ . The position of the 273-keV energy is marked by an arrow.

The 259.2-keV ground-state transition, reported in the  $\beta^-$  decay work of [18], is most likely the same as the 259.5-keV transition seen in the present work. This transition is in coincidence with the 1342.3-, 139.2-, and (weaker) 194.7-keV transitions and also with the 159-keV line. The lack of any coincidence with the 126.6- and 285.6-keV transitions suggests the placement of the 259.5-keV transition as shown in Fig. 4. This placement requires the introduction of an unobserved prompt 26.2-keV transition from the 285.7-keV level to the 259.5-keV level to account for the 259.5–1342.3 coincidence. In double gate 1342.3–159.3,  $\gamma$  intensities of 259.5- and 285.6-keV transitions are the same (within 3%). This implies that the 26.3 keV transition has total intensity comparable to the  $\gamma$  intensity of the 285.6-keV transition. Because the 26.3-keV transition competes with the 126.6-keV transition it should have the same multipolarity. Therefore, it is unlikely that the 26.3-keV transition is  $E1$ . Consequently we propose negative parity for the 259.5-keV level. We note that both the observed and unobserved coincidences define the order of transitions in the 26.6–159.3-keV cascade as shown in Fig. 4.

As far as we could check, there is no evidence for any decay from the 445.0-keV to the 159.1-keV level but a weak 286.0-keV branch from the 445.0-keV level cannot be fully excluded, because it would overlap in energy with the 285.6-keV transition and its expected coincidence conditions are very similar to that of the 285.6-keV transition.

The present, triggerless data, tagged by the absolute clock, allowed studying various time correlations. Using wide time windows we were able to show the link between the decay scheme of the  $5.1 \mu\text{s}$  isomer and its prompt feeding. To obtain the relevant spectra we sorted three-dimensional histograms with various conditions on time signals. The first histogram, called DDP, contains triple- $\gamma$  coincidences, where along the P axis prompt  $\gamma$  rays registered within time window 0–300 ns are sorted, and on the two D axes we sorted  $\gamma$  rays registered within the period from 400 to 2400 ns after the “0” time (the “0” time corresponds to the arrival time of the first prompt  $\gamma$  in the coincidence event). The second histogram, called the PPD cube, contains prompt  $\gamma$  rays on the first two axes (time window 0–300 ns) and delayed  $\gamma$  rays on the third axis (time window 400–400 ns).

Figure 6 shows four  $\gamma$  spectra obtained from the the DDP and PPD histograms by gating on prompts and delayed lines in  $^{88}\text{Br}$ . Figure 6(a) shows a spectrum double gated on the 159.1- and 111.0-keV lines on the two D axes of the DDP cube. The resulting gated spectrum contains prompt  $\gamma$  decays feeding the 270.1-keV isomer. The spectrum is dominated by the 293.6- and the 139.2-keV prompt transitions. In Fig. 6(b) a spectrum obtained from the PPD cube is shown, where the gates are set on the 293.6- and 139.2-keV lines on two P axes. In the spectrum one observes delayed  $\gamma$  transitions in the cascade deexciting the 270.1-keV isomer. The arrow marks the position of 270.1 keV, confirming the absence of the 270.1-keV direct decay of the isomer to the ground state.

In Figs. 6(c) and 6(d) we show spectra obtained from the DDP histogram with the first gate on the 159.1- or 111.0-keV line on the D axis and the second gate on the 293.6- or 139.2-keV line on the P axis, respectively. In these spectra we observe only the 111.0- and the 159.1-keV delayed  $\gamma$  transitions below the 270.1-keV isomer.

### C. Isomeric ratio of the 270.1-keV isomer

Comparing spectra from the DDP and PPP cubes (the latter sorted with 300 ns time window on all axes) we could estimate the intensity of the 111.0-keV, isomeric transition. First, in a spectrum gated on 111.0- and 159.1-keV lines of  $^{88}\text{Br}$ , on two D axes of the DDP cube we have observed prompt- $\gamma$  intensity of the 314.2- and 384.2-keV lines of the  $^{145}\text{La}$  complementary fission fragment nucleus [20]. Second, in a spectrum gated on 113.9- and 159.1-keV lines of  $^{88}\text{Br}$ , on two P axes of the PPP cube we have observed an analogous prompt- $\gamma$  intensity of the 314.2- and 384.2-keV lines of  $^{145}\text{La}$ . We note that intensities of the 314.2- and 384.2-keV lines in the two spectra are proportional to intensities of the 111.1- and 113.9-keV lines, respectively. However on the DDP cube only 23% of the isomeric intensity is observed in the D window. Taking the prompt intensity of the 113.9-keV line as a reference and making the relevant corrections, we deduced the total  $\gamma$  intensity of the 111.0-keV isomeric transition to be 154(18) in the relative units of Table I. This value allows to calculate the isomeric ratio,  $\text{iso}/(\text{iso}+\text{g.s.})$ , as defined in Ref. [19], to be 0.38(6) (the error corresponds to statistical uncertainties).

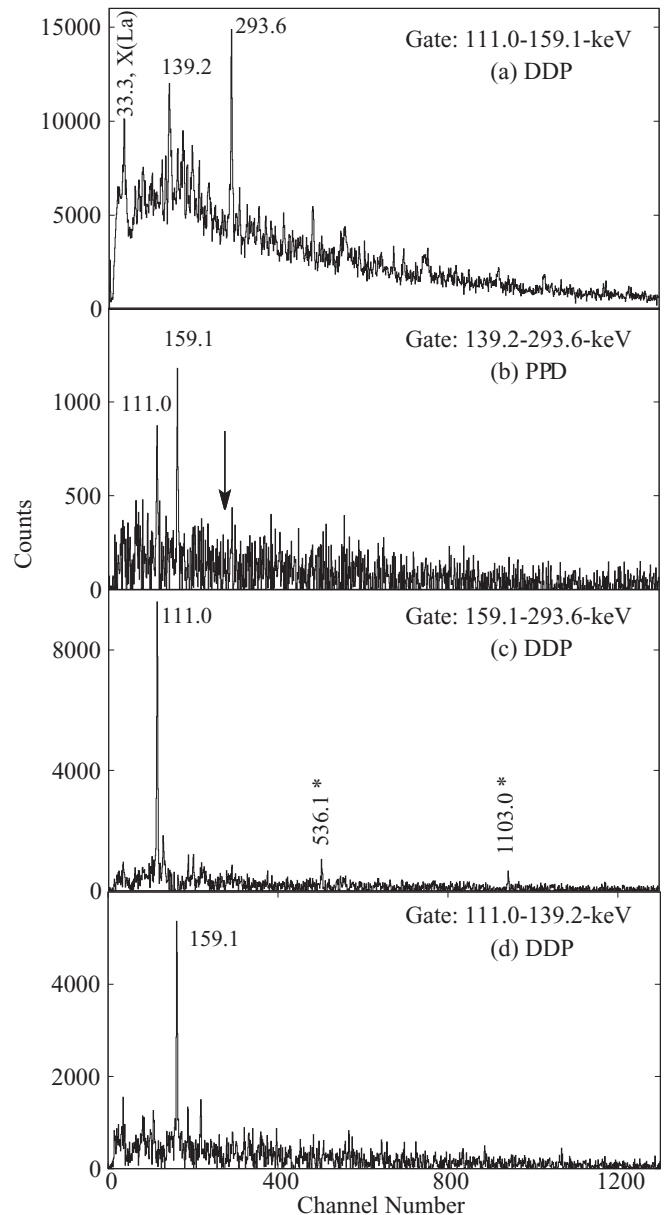


FIG. 6. Coincidence spectra gated on  $\gamma$  lines in  $^{88}\text{Br}$ , as obtained from the DDP and the PPD histograms. Energies of  $\gamma$  lines are labeled in keV. Lines marked with stars are due to contaminations. In (b) the arrow indicates the position of 270.1 keV.

### D. Half-lives measurements

Half-lives of excited levels may provide useful information on the multiplicities of their decay branchings, assisting spin and parity assignments to these levels. The present experiment, where all  $\gamma$  signals were accompanied by time tags from 100 MHz clock, provides the possibility to check half-lives of levels in the nano- to - microsecond range.

To determine half-lives of excited levels we have sorted a 3D histogram, where the energy of  $\gamma_1$  is on axis 1, the energy of  $\gamma_2$  on axis 2, and the difference of their time tags on axis 3. The range on the third axis is from  $-2.4$  to  $+2.4 \mu\text{s}$  with time



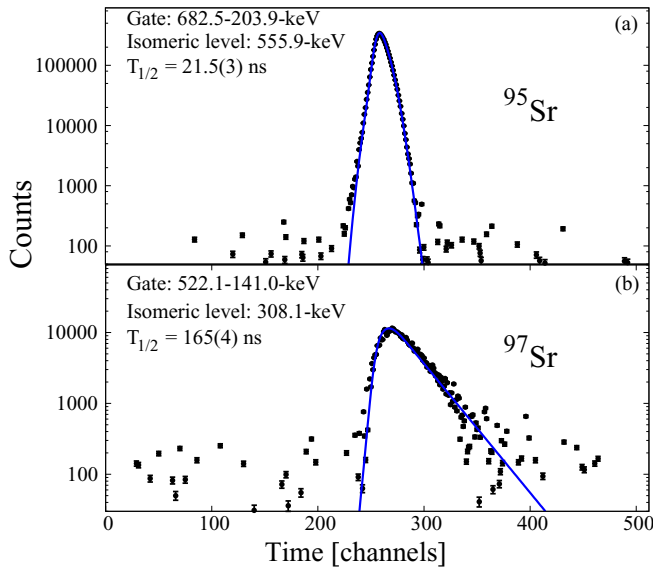


FIG. 7. (Color online) Time spectra for (a) the 21.9(5) ns, 556.8-keV isomer in  $^{95}\text{Sr}$  [21] and (b) the 169(9) ns, 308.1-keV isomer in  $^{97}\text{Sr}$  [22].

calibration of 10 ns per channel and the “zero” time in channel 256.

The prompt peak on the time axis may be complex, as discussed in Refs. [11]. It may be approximated by a Gaussian shape, but due to the large Ge detector volumes and the add-back procedure applied, the width of the distribution is large, being about 50 ns, on average. The width and the position of the prompt peak varies with  $\gamma$  energy, and for energies lower than 300 keV this “jitter” effect has to be considered.

The prompt response for the time-difference spectrum is a superposition of two prompt peaks, for  $\gamma_1$  (start) and  $\gamma_2$  (stop). We have parametrized the shape of the prompt response in the time-difference spectrum as a function of  $\gamma_1$  and  $\gamma_2$  energies using about 50 known cascades between levels with half-lives shorter than a nanosecond. The parametrization has been tested by determining several half-lives in a range from 10 to 500 ns. The deconvolution of the experimental data with the time-difference prompt peak provided half-lives that are consistent with the literature values. In Fig. 7 we show an example of such analysis for the 21.9(5)-ns, 556.8-keV isomer in  $^{95}\text{Sr}$  and the 169(9)-ns, 308.1-keV isomer in  $^{97}\text{Sr}$ . Our procedure gives half-lives of 21.5(3) and 165(4) ns for the two isomers, respectively. The new values agree with, and are more precise than, the literature values [21,22]. We tested that our analysis allows the determination of half-lives down to 7 ns, a value which we adopt as the lower limit for this method.

In  $^{88}\text{Br}$  one expects half-lives in the nanosecond range for single-particle  $E2$  transitions with energies below 300 keV and for  $M2/E3$  transitions with energies around 1 MeV. When scaled with energy (assuming a single-particle rate) the half-life of the 5.1  $\mu\text{s}$  isomer, decaying by the  $E2$  transition of 111.0 keV, translates to the partial half-life of 41 ns for the 290.8-keV,  $E2$  decay from the  $5^-$ , 563.7-keV level. Considering that the other two decays from this level, which are expected to be fast  $M1 + E2$  transitions, bear over 80% of the

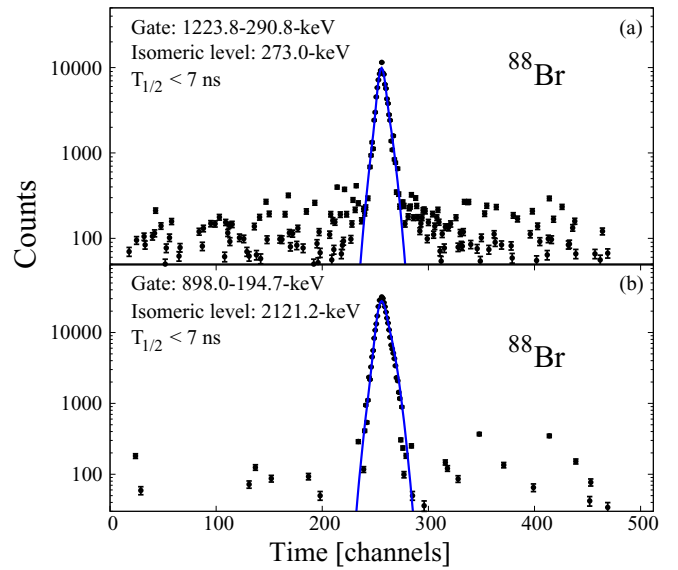


FIG. 8. (Color online) Time spectra for (a) the 273.0-keV level and (b) the 2121.2-keV level in  $^{88}\text{Br}$  as obtained in this work.

$\gamma$  intensity, one estimates the total half-life for the 563.7-keV level to be about 6 ns. The analysis of the time spectrum for the 290.8-keV decay, shown in Fig. 8(a) gives time zero, which is consistent with the upper limit of 7 ns for the method.

A similar limit applies to all other levels of  $^{88}\text{Br}$  (except the 5.1  $\mu\text{s}$  isomer) in particular for the 1787.3-, 1926.6- and 2121.2-keV levels. The analysis of the time spectrum for the 194.7-keV decay of the 2121.2-keV level is shown in Fig. 8(b). The time peak is broader than for the 290.8-keV decay in Fig. 8(a) due to larger “jitter”, but the half-life fitted is zero.

### E. Spin and parity assignments for levels in $^{88}\text{Br}$

The knowledge of spins and parities of levels is essential for their interpretation. In the present work we have measured angular correlations for  $\gamma\gamma$  cascades in  $^{88}\text{Br}$  using 28 pairs of the eight EXOGAM clover detectors mounted in the EXILL spectrometer in one plane in an octagonal geometry. This configuration provides three different angles between detectors:  $0^\circ$ ,  $45^\circ$ , and  $90^\circ$ . More details on the technique are reported in [11]. The geometry and technical details are similar to that described in our previous measurement at the PF1B facility of ILL [16].

To find intensities in  $\gamma\gamma$  cascades at the three angles we sorted a 3D, “ $\gamma$ - $\gamma$ -angle” histogram. The experimental angular correlations were then analyzed using programs developed in Ref. [16], based on the formalism of Krane, Steffen, and Wheeler [23]. The theoretical formula for the angular correlation function between two consecutive  $\gamma$  transitions in a cascade from an unoriented state with spin  $J_i$ , through an intermediate level with spin  $J'$ , to the final level with spin  $J_f$  can be expressed as a series of Legendre polynomials,

$$W(\theta) = \sum_k A_k P_k(\cos \theta) \quad (1)$$

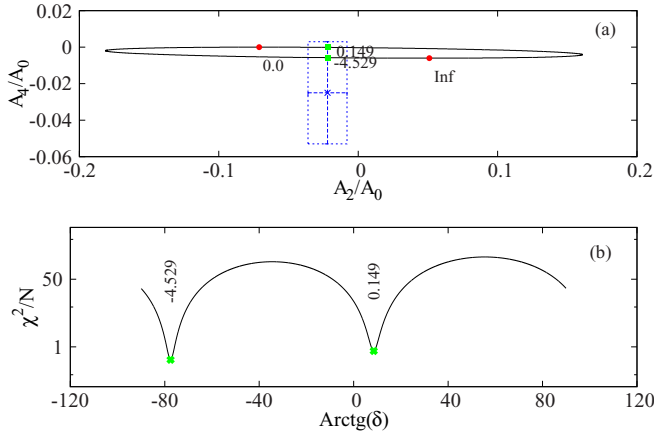


FIG. 9. (Color online) Angular correlation analysis for the 111.0–159.1-keV cascade in  $^{88}\text{Br}$ .

where  $\theta$  is an angle between the directions of  $\gamma_1$  and  $\gamma_2$  transitions in the cascade.  $P_k$  are the Legendre polynomials of rank  $k$ , which is an even integer number and runs from zero to the least of  $2J'$ ,  $2L_1$ , or  $2L_2$ . Variables  $L_1$ ,  $L'_1$  and  $L_2$ ,  $L'_2$  are the maximal multiplicities of  $\gamma_1$  and  $\gamma_2$ , respectively. Values of  $A_k$  coefficients, which depend on the  $J_i$ ,  $J'$ , and  $J_f$  spins and on the  $L_1$ ,  $L'_1$ ,  $L_2$ , and  $L'_2$  multiplicities can be calculated for various hypothesis of spins and multiplicities in the concerned cascade using programs from Ref. [16].

As an example, in Fig. 9 we present angular correlation analysis for the 111.0–159.1-keV cascade depopulating the 5.1  $\mu\text{s}$  isomer in  $^{88}\text{Br}$ . For the 270.1- and 159.1-keV levels and the ground state we have assumed spins of  $4^-$ ,  $2^-$ , and  $1^-$ , respectively. Part (b) of Fig. 9 presents a plot of the  $\chi^2$  function per degree of freedom. The “ellipse” in part (a) represents theoretical values of  $A_2/A_0$  and  $A_4/A_0$  coefficients for the assumed spin hypothesis as a function of the mixing ratio,  $\delta$ , which varies from 0 to  $\pm\infty$  (red dots) along the two branches of the “ellipse”. The experimental values of  $A_2/A_0$  and  $A_4/A_0$  with their error bars are presented by the rectangle box (blue). As shown in Fig. 9, there are two solutions, with the mixing coefficient of the 159.1-keV transition  $\delta = 0.149(41)$  or  $\delta = -4.51(-1.1, +0.73)$  (green dots). As in the above example, the experimental value of  $A_4/A_0$  is often not precise enough to determine one solution. When possible, other cascades were analyzed to find a unique value of  $\delta$ . In addition we have used the well-documented observation of the predominant population of yrast levels in the fission process [24] as well as arguments derived from the observed decay branchings.

Results of the angular correlation analysis for  $\gamma\gamma$  cascades in  $^{88}\text{Br}$  are presented in Table II, and below we discuss spin and parity assignments for levels in  $^{88}\text{Br}$ .

### 1. The ground state and the 159.1- and 270.1-keV levels

These levels, reported previously [19], were assigned spins and parities ( $1^-$ ), ( $2^-$ ), and ( $4^-$ ), respectively. Spin ( $1^-$ ) for the ground state is supported by semi-empirical calculations done in Ref. [19]. Angular correlations in Table II are consistent

TABLE II. Normalized experimental angular correlation coefficients and the corresponding mixing coefficients for  $\gamma$  transitions in  $^{88}\text{Br}$ .

Cascade	$A_2/A_0$	$A_4/A_0$	Spin hypothesis	$\delta(\gamma^a)$
111.0–159.1 <sup>a</sup>	−0.022(14)	−0.025(28)	4 → 2 → 1	0.15(4)
			4 → 2 → 1	−4.5( $^{+0.7}_{-1.0}$ )
113.9 <sup>a</sup> –159.1	0.009(12)	−0.042(25)	3 → 2 → 1	0.04(7)
			3 → 2 → 1	4.8( $^{+2.6}_{-1.3}$ )
			3 → 3 → 2	13.3( $^{+8.1}_{-6.1}$ )
172.0 <sup>a</sup> –113.9	0.055(25)	−0.022(50)	4 → 3 → 2	−0.04(6)
			4 → 3 → 2	13.3( $^{+6.6}_{-10.0}$ )
			3 → 3 → 2	0.64(12)
			3 → 3 → 2	−13.3( $^{+6.6}_{-10.0}$ )
159.3 <sup>a</sup> –285.6	0.089(13)	0.023(29)	4 → 3 → 1	0.5(1)
			4 → 3 → 1	7.8( $^{+4.6}_{-2.3}$ )
118.7 <sup>a</sup> –172.0	0.066(31)	0.054(68)	5 → 4 → 3	0
			4 → 4 → 3	0.90( $^{+32}_{-20}$ )
			4 → 4 → 3	13.3( $^{+8.3}_{-Inf}$ )
			4 → 4 → 3	0
1342.3 <sup>a</sup> –172.0	−0.100(47)	0.000(95)	5 → 4 → 3	0.31(14)
			5 → 4 → 3	2.5(9)
			6 → 4 → 3	0
			7 → 4 → 3	0
			7 → 4 → 3	0
139.2 <sup>a</sup> –1342.3	0.149(55)	−0.01(12)	7 → 6 → 4	0.41( $^{+18}_{-14}$ )
			6 → 5 → 4	0.26( $^{+11}_{-9}$ )

<sup>a</sup>Indicates mixed  $\gamma$  transition.

with two spin hypothesis for the isomeric cascade,  $4 \rightarrow 2 \rightarrow 1$  and  $4 \rightarrow 2 \rightarrow 3$ . Due to the fact that there is no direct decay from the 270.1-keV isomer to the ground state, we reject the  $4 \rightarrow 2 \rightarrow 3$  solution. Assuming spin and parity  $1^-$  for the ground state and taking stretched quadrupole multiplicity for the 111.0-keV transition, as found in Ref. [19] based on the internal coefficient measurement, we determined for the 159.1-keV transition a mixed dipole-quadrupole character with mixing coefficients  $\delta = 0.149(41)$  or  $\delta = -4.5(-1.0, +0.7)$ . Such large mixing coefficients exclude  $E1 + M2$  character for the 159.1-keV transition. Therefore, this transition should have an  $M1 + E2$  multipolarity, which agrees with the internal conversion coefficient measurement for the 159.1-keV transition [19]. It may also be mentioned that  $\delta = -4.5(-1.1, +0.7)$  would contradict with the measured conversion coefficient [19], so we reject this possibility.

We note that in recent compilation [25] spin ( $2^-$ ) is proposed for the ground state of  $^{88}\text{Br}$ . As will be discussed further in Sec. III, our data is in favor of spin  $1^-$  for the ground state and spin  $4^-$  for the isomer.

### 2. The 273.0-keV level

For the 273.0-keV level we propose spin  $I = 3$  based on the prompt character of the 113.9-keV transition. This points to the  $\Delta I \leq 1$  character of the 113.9-keV transition. On the other hand, the nonobservation of the 273.0-keV decay to the ground state points to the  $\Delta I > 1$  character of the 273.0-keV (unobserved) decay.

For the 113.9-keV transition a mixed dipole-quadrupole solution with  $\delta = 0.04(-0.07)$  or  $\delta = 4.7(-1.3, +2.6)$  is obtained when assuming spin 3 for the 273.0-keV level

and mixing  $\delta = 0.149$  for the 159.1-keV transition. When assuming spin 3 for the 273.0-keV level and mixing  $\delta = -4.5$  for the 159.1-keV transition one obtains one solution with  $\delta = 0.04(7)$  for the 113.9-keV transition.

Summarizing, we propose spin 3 for the 273.0-keV level. The  $\delta = 0.04(7)$  solution, which is nearly zero, does not allow us to reject  $M1/E2$  character of the 113.9-keV transition although a pure  $E1$  multipolarity is less likely due to the prompt character of the 113.9-keV decay on one hand and the absence of strong octupole correlations in this region on the other hand. Therefore negative parity is preferred for the 273.0-keV level

One may argue that the  $\delta = 4.7(-1.3, +2.6)$  value for the 113.4-keV transition is less likely because otherwise this transition is an almost pure  $E2$ , resulting in a long half-life of the 273.0-keV level, which is not observed.

### 3. The 285.7- and 445.0-keV levels

Our angular correlations are not compatible with spin 5 for the 445.0-keV level. Taking for the 113.9-keV transition  $\delta = 0.04(7)$  we obtain for the 172.0-keV transition  $\delta = -0.04(6)$  or  $\delta = 13.3(-6.1, +81.0)$  when assuming spin 4 for the 445.0-keV level, and  $\delta = 0.64(12)$  or  $\delta = -13.3(-1000, +6.6)$  when assuming spin 3 for this state.

Spin 4 is favored by the “yrast-population” argument. Spin 3 is unlikely because of no decay to the 159.1-keV level. Therefore we propose spin 4 for the 445.0-keV level.

Spin 4 solution for the 445.0-keV level is consistent with angular correlation analysis for the 285.6–159.3-keV cascade when assuming spin 3 for the 285.7-keV level. Spin 2 for this level is unlikely considering prompt character of the 159.3-keV decay. With spin 3 the 285.6-keV transition has stretched quadrupole multipolarity. Then for the 159.3-keV transition  $\delta = 0.5(1)$  or  $\delta = 7.8(-2.3, +4.6)$  is obtained. The nonzero  $\delta$  suggests an  $M1 + E2$  character of the 159.3-keV transition and negative parity of the 285.7-keV level.

### 4. The 259.5-keV level

The presence of the 26.3-keV decay from the 285.7-keV level restricts spin of the 259.5-keV level to 2, 3, or 4. Negative parity is favored because the 26.3-keV decay has rather an  $M1 + E2$  than an  $E1$  multipolarity due to its prompt character. The  $4^-$  solution is unlikely because of the prompt decay of the 259.5-keV level to the  $1^-$  ground state. Also  $3^-$  solution is unlikely because the 445.0-keV level does not decay to the 259.5-keV level. Therefore we propose spin and parity  $2^-$  for the 259.5-keV level.

### 5. The 563.7-keV level

For the 118.7-172.0-keV cascade the angular correlations are consistent with spin 3, 4, or 5 for the 563.7-keV level. Spin 3 is unlikely because no decay is observed to levels with spin 2. Furthermore, in the case of spin 3 the 563.7-keV level would be rather non-yrast despite its strong population. Assuming spin 4 for the 563.7-keV level we obtain mixed dipole-quadrupole multipolarity of the 118.7-keV transition with large mixing coefficients  $\delta = 0.90(-20, +32)$  or  $\delta = -13.3(-200, +8.3)$ . We also note that there is no decay to

the 285.7-keV level, with proposed spin  $3^-$ . For the spin 5 hypothesis a dipole character for the 118.7-keV transition is derived, which is more likely, considering the prompt character of this transition.

Summarizing, spin 5 is preferred for the 563.7-keV level. In this case its parity has to be negative, because of the prompt, 290.8-keV decay to the 273.0-keV level, which has spin and parity  $3^-$ .

## 6. The 1787.3-keV level

With spin 3 for the 273.0-keV level, the angular correlation for the 172.0–1342.3-keV cascade provides three spin solutions for the 1787.3-keV level:  $I = 5, 6, \text{ or } 7$ . Taking an  $M1/E2$  character with  $\delta = -0.04$  for the 172.0-keV transition, as discussed above, and assuming spin 5 for the 1787.3-keV level, we deduce for the 1342.3-keV transition mixing ratios  $\delta = 0.31(14)$  or  $\delta = 2.5(9)$ . Angular correlations indicate a stretched (unmixed) quadrupole character for the 1342.3-keV transition when assuming spin 6 for the 1787.3-keV level, and a pure octupole multipolarity when assuming spin 7 for this level.

With mixing coefficient  $\delta = 0.31(14)$  or  $\delta = 2.5(9)$  the 1342.3-keV transition can have either  $M1 + E2$  or  $E1 + M2$  multipolarity. In this case spin and parity of the the 1787.3-keV level should be either  $5^-$  or  $5^+$ . One may argue that the  $5^-$  option is less likely because of no decay to any of the  $3^-$  levels, whereas an  $E2$  branch should be quite strong at this transition energy. In Table III single-particle estimates of partial half-lives for several discussed decay branches are shown, to help the discussion. In addition we use the information from compilations of hindrance of electromagnetic rates in nuclei [26].

Spin 6 for the 1787.3-keV level is possible, considering the observed branching ratios. We propose positive parity for the 1787.3-keV level, as discussed in the next section.

The spin 7 solution should be accompanied by the positive parity because negative parity would mean an  $M3$  multipolarity of the 1342.3-keV transition and a partial half-life of dozens of microseconds, which is not observed. Positive parity and spin 7 for the 1787.3-keV level should be considered, because  $E3$  decays with rates of 1 W.u. are known in  $^{87}\text{Rb}$  and  $^{88}\text{Rb}$  and the 1494-keV,  $E3$  decay in  $^{86}\text{Br}$  has a prompt character [27]. However, the intensity ratio of the 1342.3- and 1223.8-keV transitions in  $^{88}\text{Br}$  is rather inconsistent with the  $B(M2)/B(E3)$  branching ratios observed in  $^{86}\text{Br}$  and  $^{88}\text{Rb}$ . Assuming that the 1223.8-keV decay in  $^{88}\text{Br}$  has an  $M2$  multipolarity and the rate of 0.1 W.u. and the 1342.3-keV decay has an  $E3$  multipolarity at the rate of 1 W.u., as observed in  $^{88}\text{Rb}$  [27], we conclude that the 1223.8-keV transition should be about 60 times more intense than the 1342.3-keV transition, while the two transitions have comparable intensities (see Table I).

## 7. The 1926.5-keV level

Starting with spin  $I$  of the 1787.3-keV level two solutions,  $I + 1$  and  $I + 2$  are obtained for the spin of the 1926.5-keV level from angular correlations of the 139.2–1342.3-keV cascade. The  $I + 2$  solution means that that the 139.2-keV

TABLE III. Single-particle estimates of partial half-lives for decay branches of the 1787.3-keV level in  $^{88}\text{Br}$ , for various multipolarities  $E1$ ,  $E2$ ,  $E3$ ,  $M1$ , and  $M2$ . See text for further explanation.

Transition energy (keV)	$T_{1/2}$ (s) $E1$	$T_{1/2}$ (s) $E2$	$T_{1/2}$ (s) $E3$	$T_{1/2}$ (s) $M1$	$T_{1/2}$ (s) $M2$
773.5	$1.07 \times 10^{-15}$	$1.28 \times 10^{-10}$	$2.31 \times 10^{-5}$	$6.93 \times 10^{-14}$	$8.26 \times 10^{-9}$
1223.8	$2.70 \times 10^{-16}$	$1.29 \times 10^{-11}$	$9.32 \times 10^{-7}$	$1.75 \times 10^{-14}$	$8.33 \times 10^{-10}$
1342.3	$2.05 \times 10^{-16}$	$8.11 \times 10^{-12}$	$4.88 \times 10^{-7}$	$1.33 \times 10^{-14}$	$5.25 \times 10^{-10}$
1517.2	$1.42 \times 10^{-16}$	$4.40 \times 10^{-12}$	$2.07 \times 10^{-7}$	$9.18 \times 10^{-15}$	$2.84 \times 10^{-10}$

transition should be a stretched quadrupole. This transition is of prompt character and an  $M2$  multipolarity can be rejected. Also an  $E2$  multipolarity would lead to a half-life of about a microsecond for the 1926.5-keV level, which is not observed. We also note that an  $E1$  multipolarity would mean negative parity of the 1926.5-keV level. In such a case there should be high-energy  $M1$  or  $E2$  decays, very competitive to an  $E1$  decay of 139 keV, which is not observed. Therefore we propose an  $M1 + E2$  character of the 139.2-keV transition and spin  $I + 1$  with positive parity for the 1926.5-keV level.

With spin  $6^+$  for the 1787.3-keV level and spin  $7^+$  for the 1926.5-keV level,  $\delta = 0.41(-14, +18)$  or  $\delta = 2.1(-6, +9)$  is obtained for the 139.2-keV transition. With spin  $5^+$  for the 1787.3-keV level and spin  $6^+$  for the 1926.5-keV level,  $\delta = 0.26(-9, +11)$  or  $\delta = 3.1(-9, +13)$  is obtained for the 139.2-keV transition. In both cases the large mixing supports the  $M1 + E2$  character of the 139.2-keV transition.

### 8. Other levels

The prompt character of the 194.7-keV transition, the yrast-population argument, and the absence of the decay to the 1787.3-keV level suggest spin one unit higher than the spin of the 1926.5-keV level. Positive parity for the 2121.2-keV level is preferred because of the observed decay branch.

All the remaining transitions are prompt. Using this observation, the yrast-population argument, and the observed branchings, we tentatively propose spins and parities for some other levels in  $^{88}\text{Br}$  as shown in Fig. 4. In particular for the 1446.2- and 1633.9-keV levels, negative parity is favored by the absence of any link with the 1787.3-keV level.

## III. DISCUSSION

Low-spin structure of  $^{88}\text{Br}$  should be similar to that of the odd-odd isotope  $^{86}\text{Br}$ . With one valence proton-neutron pair,  $^{86}\text{Br}$  is a simple nucleus with the odd proton occupying the  $2p_{3/2}$  orbital and the odd neutron in the  $2d_{5/2}$  orbital. The proton may be promoted to the  $1f_{5/2}^{-1}$  orbital, which is close in energy. Therefore, one expects in  $^{86}\text{Br}$  two overlapping multiplets corresponding to the particle-particle  $(\pi p_{3/2}, \nu d_{5/2})_j$  and particle-hole  $(\pi f_{5/2}^{-1}, \nu d_{5/2})_j$  configuration, with spin  $j$  ranging from  $1^-$  to  $4^-$  and from  $0^-$  to  $5^-$ , respectively. At higher energy, where the odd proton is elevated to the  $1g_{9/2}$  orbital, the  $(\pi g_{9/2}, \nu d_{5/2})_j$  particle-particle multiplet is expected with spin  $j$  in a range from  $2^+$  to  $7^+$ . Such excitations have been recently reported by Porquet *et al.* [27] in a measurement of yrast excitations of  $^{86}\text{Br}$  and  $^{88}\text{Br}$ .

In the next two sections, we will use the results of Ref. [27], and in particular the identification of the characteristic  $(\pi g_{9/2}, \nu d_{5/2})_{7^+}$  configuration, to give a rough idea how to interpret excited levels in  $^{88}\text{Br}$ . An intriguing question is whether in  $^{88}\text{Br}$  one could recognize any new phenomena, not seen in  $^{86}\text{Br}$ , which are related to the seniority-3 excitations in the  $(\nu d_{5/2})_j^3$  multiplet, observed at  $N = 53$  [3].

### A. $\pi p_{3/2} \nu d_{5/2}$ and $\pi f_{5/2}^{-1} \nu d_{5/2}$ proton-neutron multiplets in $^{88}\text{Br}$

We assume, after Ref. [19], that the ground state and the isomer at 270.1 keV in  $^{88}\text{Br}$  belong to the  $(\pi p_{3/2}, \nu d_{5/2})_j$  multiplet. The observation of stretched  $E2$  transition from the  $(3^-)$  level at 285.7 keV to the ground state and the lack of analogous decay from the  $(3^-)$  level at 273.0 keV suggests that the 285.7-keV level belongs to the  $(\pi p_{3/2}, \nu d_{5/2})_j$  multiplet. The 285.7-keV level decays to both  $(2^-)$  levels, at 159.1 and 259.5 keV. Considering the energies of both decays, the 126.6-keV transition should be two orders of magnitude more intense than the 26.2-keV branch, if there were no structural effect. Because the total intensities of both branches are comparable, we propose that the 259.5-keV level belongs to the  $(\pi p_{3/2}, \nu d_{5/2})_j$  multiplet.

The four levels assigned to the  $(\pi p_{3/2}, \nu d_{5/2})_j$  multiplet exhaust the list of its members. Therefore other low-energy levels observed in  $^{88}\text{Br}$  should belong to the  $(\pi f_{5/2}^{-1}, \nu d_{5/2})_j$  configuration. The new level at 563.7 keV, to which we assign spin  $(5^-)$  is a good candidate for the highest-spin member of the  $(\pi f_{5/2}^{-1}, \nu d_{5/2})_j$  multiplet. It is observed at similar excitation energy as the analogous  $5_1^-$  level in  $^{86}\text{Br}$ , about 300 keV above the  $4_1^-$  level. The 563.7-keV level decays preferably to the 445.0-keV level, considering energy-scaled intensities  $[B(M1)]$  of its decay branches. It has also an  $E2$  decay branch to the 273.0-keV level. This suggests that the 273.0- and 445.0-keV levels belong to the  $(\pi f_{5/2}^{-1}, \nu d_{5/2})_j$  multiplet. We propose that the 159.1-keV level also belongs to the  $(\pi f_{5/2}^{-1}, \nu d_{5/2})_j$  multiplet.

As the first verification of this picture we compare experimental levels in  $^{88}\text{Br}$  to semiempirical estimates of excitation energies within the  $(\pi p_{3/2}, \nu d_{5/2})$  and  $(\pi f_{5/2}^{-1}, \nu d_{5/2})$  multiplets, calculated in a similar way as in Ref. [19], using the formalism described in Refs. [28,29]. In Table IV we show our calculations for the  $(\pi p_{3/2}, \nu d_{5/2})$  multiplet reported in Ref. [19]. Residual interactions are calculated, as in Ref. [19], applying Pandya transformation [28,31] to the interactions in the  $(\pi p_{3/2}, \nu d_{5/2})$  multiplet in  $^{88}\text{Rb}$  [27]. The interactions in the  $(\pi p_{3/2}, \nu d_{5/2})$  multiplet in Table IV are the same as those



TABLE IV. Semiempirical estimates of excitation energies within the  $\pi p_{3/2} \nu d_{5/2}$  multiplet in  $^{88}\text{Br}$ . See text for further explanation.

Spin $I$	Excitation in $^{88}\text{Rb}$ [30] (keV)	$V_{\text{res}}(\pi p_{3/2}^{-1} \nu d_{5/2})$ in $^{88}\text{Rb}$ (keV)	$V_{\text{res}}(\pi p_{3/2} \nu d_{5/2})$ from Pandya (keV)	$E_{\text{exc}}^{\text{cal}}$ $^{88}\text{Br}$ (keV)
$1^-$	196	472	-649	0
$2^-$	0	276	-499	150
$3^-$	28	304	-277	372
$4^-$	268	544	-382	267

calculated in Ref. [27], except for the  $1^-$  level (996 keV in Ref. [27], which would not fit  $^{88}\text{Br}$  at all).

The 267-keV energy calculated for the  $4^-$  isomer, relative to the  $1^-$  ground state, is the same as in Ref. [19]. Also the  $3^-$  level has the same calculated energy (though it does not fit well any of the two experimental  $3^-$  states proposed at 273.0 and 285.6 keV). The  $2^-$  level we calculate at 150 keV, which would fit better the  $2_1^-$  experimental level at 159 keV, while we assigned it to the  $\pi f_{5/2}^{-1} \nu d_{5/2}$  configuration (the 209-keV energy calculated in Ref. [19] would better fit the 259.6-keV experimental level, which we assigned to the  $\pi p_{3/2} \nu d_{5/2}$  configuration). It is likely that this inconsistency indicates the accuracy limits of such semiempirical estimates and the configuration assignments based on the observed branchings. A schematic comparison of experimental and calculated energies in the  $(\pi p_{3/2}, \nu d_{5/2})$  multiplet of  $^{88}\text{Br}$  is shown in Fig. 10.

When taking the interactions within the  $(\pi f_{5/2}^{-1}, \nu d_{5/2})$  multiplet in  $^{88}\text{Rb}$ , also reported in Ref. [27], and applying them to  $^{88}\text{Br}$  one gets energies of 564, 178, 228, and 200 keV for the  $5^-$ ,  $4^-$ ,  $3^-$ , and  $2^-$  levels, respectively (normalized to the experimental  $5^-$  level). Analogous energies are 564, 233, 42, and -6 keV, when taking the interactions within the  $(\pi f_{5/2}^{-1}, \nu d_{5/2})$  multiplet in  $^{86}\text{Br}$  reported in Table 9 of Ref. [27]. Again, discrepancies indicate the accuracy limit of semiempirical estimates. Schematic comparison of experimental and calculated energies in the  $(f_{5/2}^{-1}, \nu d_{5/2})$  multiplet of  $^{88}\text{Br}$  is shown in Fig. 10. For the calculated values we show the average of the two calculations mentioned.

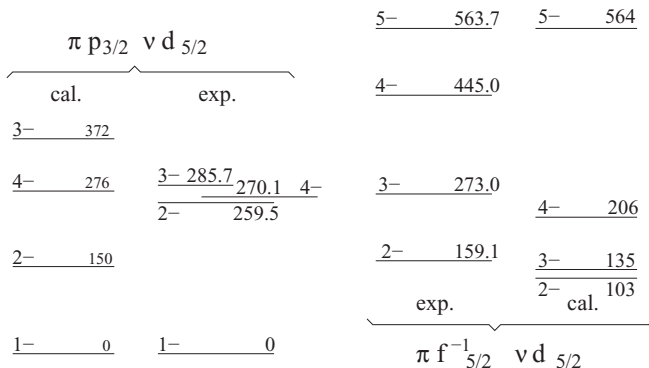


FIG. 10. Proton-neutron multiplets in  $^{88}\text{Br}$ . See text for further explanation.

Summarizing, the semiempirical estimates reproduce rough features, as the repulsive interaction in the  $(\pi f_{5/2}^{-1}, \nu d_{5/2})$  multiplet and the attractive interaction in the  $(\pi p_{3/2}, \nu d_{5/2})$  multiplet in  $^{88}\text{Br}$ . The estimates for both multiplets suggest a low-lying  $4^-$  level, though only in the  $(\pi p_{3/2}, \nu d_{5/2})$  multiplet does it become a spin trap. We also note that all low-spin levels observed in  $^{88}\text{Br}$  can be accounted for by the two multiplets, similarly as in  $^{86}\text{Br}$ . Thus, the present study does not answer the question if in  $^{88}\text{Br}$  the three neutrons in the  $\nu d_{5/2}$  orbital produce at low excitation a doublet of close lying,  $3/2^+$  and  $5/2^+$  states due to the  $j-1$  anomaly. If present, such a doublet should increase the number of low-lying proton-neutron excitations in  $^{88}\text{Br}$  as compared to  $^{86}\text{Br}$ . It is of interest to perform detailed measurements, particularly  $\beta$  decay of  $^{88}\text{Se}$ , to check whether in  $^{88}\text{Br}$  there are any additional low-energy, low-spin excitations.

### B. $\pi g_{9/2} \nu d_{5/2}$ and $\pi g_{9/2} \nu g_{7/2}$ proton-neutron multiplets in $^{88}\text{Br}$

When elevating the odd proton to the  $g_{9/2}$  orbital, one expects another maximum-aligned configuration,  $[\pi g_{9/2} \nu (d_{5/2})_{5/2}^3]_{7^+}$ . There, the purity of the  $\pi g_{9/2}$  intruder may favour the  $[\pi g_{9/2} \nu (d_{5/2})_{5/2}^3]_{6^+}$  anomalous coupling.

We have performed a semiempirical calculation described in Ref. [32], which uses excitation energies, and works well for maximum-aligned configurations also in complex, odd-odd nuclei [33]. In this method the excitation energy in the nucleus with three particles is calculated from excitation energies of simpler, one- and two-particle configurations in the neighboring nuclei according to the formula

$$E_{1,2,3} = \sum_{i,j} E_{i,j} - \sum_i E_i + W \quad (2)$$

where  $W$ , the mass window, is a sum of nuclear masses of these neighboring nuclei added (subtracted) for nuclei with even (odd) number of particles. The decomposition of the three-particle configuration of interest in  $^{88}\text{Br}$  into one- and two-particle configurations is shown in part (a) of Fig. 11, where we also show other data used for calculating the energy of the  $7^+$  level in  $^{88}\text{Br}$ . In each box there is the configuration considered in a given isotope, with its spin, parity, excitation energy, and the mass deficit for the ground state of the isotope (in keV), taken from the recent compilation [34].

For the eight nuclei in part (a) of Fig. 11 the mass window is  $W = 310(22)$  keV and the estimated energy of the  $[\pi g_{9/2} \nu (d_{5/2})^3]_{7^+}$  coupling is 1646(70) keV. The error comprises uncertainties of the mass window and the excitation energy of the  $\pi g_{9/2} \nu (d_{5/2})^2$  level in  $^{87}\text{Br}$ , estimated at 1480(50) keV, based on the  $\pi g_{9/2}$  excitation in  $^{85}\text{Br}$  and  $^{87}\text{Rb}$ , observed at 1860 and 1578 keV, respectively, and the  $\pi g_{9/2} \nu (d_{5/2})^2$  level in  $^{89}\text{Rb}$  seen at 1195 keV. With the same data and the  $[\nu (d_{5/2})^2 \nu d_{5/2}]_{3/2^+}$  configuration for the ground state in  $^{87}\text{Se}$  one estimates the energy of the  $[\pi g_{9/2} \nu (d_{5/2})^3]_{6^+}$  coupling in  $^{88}\text{Br}$  at 1554 keV.

Because the  $[\pi f_{5/2}^{-1} \nu (d_{5/2})_{5/2}^3]_{5^-}$  level in  $^{88}\text{Br}$  is expected to be unmixed we have also estimated its excitation energy. The relevant data are shown in part (b) of Fig. 11. For the  $(\pi f_{5/2}^{-1} \nu (d_{5/2})^2)_{5/2^-}$  level in  $^{87}\text{Br}$  we assumed energy 0 keV,

(a)

<sup>85</sup> Br	<sup>86</sup> Br	<sup>87</sup> Br	<sup>88</sup> Br
$\pi g_{9/2}$	$\pi g_{9/2} \nu d_{5/2}$	$\pi g_{9/2} \nu (d_{5/2})^2$	$\pi g_{9/2} \nu (d_{5/2})^2 \nu d_{5/2}$
9/2 <sup>+</sup> , 1860 -78575(3)	7 <sup>+</sup> , 1624 -75632(3)	9/2 <sup>+</sup> , (1480) -73892(3)	7 <sup>+</sup> , E <sub>exc</sub> =? -70716(3)
<sup>84</sup> Se	<sup>85</sup> Se	<sup>86</sup> Se	<sup>87</sup> Se
CORE	$\nu d_{5/2}$	$\nu (d_{5/2})^2$	$\nu (d_{5/2})^2 \nu d_{5/2}$
0 <sup>+</sup> , 0 -75947(2)	5/2 <sup>+</sup> , 0 -72413(3)	0 <sup>+</sup> , 0 -70503(3)	5/2 <sup>+</sup> , 92 -66426(2)

(b)

<sup>86</sup> Kr	<sup>87</sup> Kr	<sup>88</sup> Kr	<sup>89</sup> Kr
CORE	$\pi p_{3/2} \nu d_{5/2}$	$\pi p_{3/2} \nu (d_{5/2})^2$	$\pi p_{3/2} \nu (d_{5/2})^2 \nu d_{5/2}$
0 <sup>+</sup> , 0 -83265(1)	5/2 <sup>+</sup> , 0 -80709(1)	0 <sup>+</sup> , 0 -79691(3)	5/2 <sup>+</sup> , 29 -76536(2)
<sup>85</sup> Br	<sup>86</sup> Br	<sup>87</sup> Br	<sup>88</sup> Br
$\pi f_{5/2}^{-1}$	$\pi f_{5/2}^{-1} \nu d_{5/2}$	$\pi f_{5/2}^{-1} \nu (d_{5/2})^2$	$\pi f_{5/2}^{-1} \nu (d_{5/2})^2 \nu d_{5/2}$
5/2 <sup>-</sup> , 345	5 <sup>-</sup> , 575	5/2 <sup>+</sup> , (0)	5 <sup>-</sup> , E <sub>exc</sub> =?

(c)

<sup>85</sup> Br	<sup>86</sup> Br	<sup>87</sup> Br	<sup>88</sup> Br
$\pi g_{9/2}$	$\pi g_{9/2} \nu g_{7/2}$	$\pi g_{9/2} \nu (d_{5/2})^2$	$\pi g_{9/2} \nu (d_{5/2})^2 \nu g_{7/2}$
9/2 <sup>+</sup> , 1860	8 <sup>+</sup> , (2687)	9/2 <sup>+</sup> , (1480)	8 <sup>+</sup> , E <sub>exc</sub> =?
<sup>84</sup> Se	<sup>85</sup> Se	<sup>86</sup> Se	<sup>87</sup> Se
CORE	$\nu g_{7/2}$	$\nu (d_{5/2})^2$	$\nu (d_{5/2})^2 \nu g_{7/2}$
0 <sup>+</sup> , 0	7/2 <sup>+</sup> , 1115	0 <sup>+</sup> , 0	7/2 <sup>+</sup> , 836

FIG. 11. Input data for the semiempirical estimate of the excitation energy in <sup>88</sup>Br for the  $[\pi g_{9/2} \nu (d_{5/2})^3]_{7^+}$  coupling (a), the  $[\pi f_{5/2}^{-1} \nu (d_{5/2})^3]_{5^-}$  coupling (b), and the  $[\pi g_{9/2} \nu (d_{5/2})^2 g_{7/2}]_{8^+}$  coupling (c). See text for further explanation.

because the 5/2<sup>-</sup> spin and parity assignment to the ground state of <sup>87</sup>Br is more likely [35,36] than the 3/2<sup>-</sup> assignment proposed earlier [37,38]. For this case we get the mass window  $W = 366(24)$  keV and estimate the excitation energy for the  $[\pi f_{5/2}^{-1} \nu (d_{5/2})^3]_{5^-}$  level to be 625 keV, not far from the experimental value of 564 keV.

The above estimates qualitatively account for the 5<sup>-</sup>, 6<sup>+</sup>, and 7<sup>+</sup> experimental levels proposed in this work. The distance between the calculated 5<sup>-</sup> and 7<sup>+</sup> levels is similar to that seen in <sup>86</sup>Br [27]. The observation of the 6<sup>+</sup> level in <sup>88</sup>Br, which does not have a counterpart in <sup>86</sup>Br, suggests that the 6<sup>+</sup> and 7<sup>+</sup> levels in <sup>88</sup>Br correspond to the  $\nu (d_{5/2})^3_{j,j-1}$  anomalous doublet coupled to the  $g_{9/2}$  proton.

If the 6<sup>+</sup> and 7<sup>+</sup> levels calculated at 1554 and 1646 keV correspond to experimental levels at 1787.3 and 1926.5 keV, respectively, then the 2121.2-keV levels should have spin 8<sup>+</sup>. The reproduction of such spin requires the promotion of the odd neutron to the  $g_{7/2}$  orbital. The excitation energy of the resulting  $[\pi g_{9/2} \nu (d_{5/2})^2 g_{7/2}]_{8^+}$  coupling can be estimated using input data shown in part (c) of Fig. 11. The mass window is 310(22) keV. The  $g_{7/2}$  excitation in <sup>85</sup>Se is at 1115 keV [39] and for the 7/2<sup>+</sup> level in <sup>87</sup>Se we adopt the 836-keV value [3]. For the 8<sup>+</sup> excitation in <sup>86</sup>Br we assume the 2687-keV level, decaying to the 7<sup>+</sup> level. The energy of the  $\pi g_{9/2} \nu (d_{5/2})^2$  level in <sup>87</sup>Br is 1480(50) keV, as discussed above. With this input the  $[\pi g_{9/2} \nu (d_{5/2})^2 g_{7/2}]_{8^+}$  configuration in <sup>88</sup>Br is predicted at 2338 keV.

The above result is in qualitative agreement with the assignment of spin 8<sup>+</sup> to the 2121.2-keV level. However, the uncertainty is high, due to various assumptions, especially about the 8<sup>+</sup> excitation in <sup>86</sup>Br. We also note that the distance between the calculated 8<sup>+</sup> and 7<sup>+</sup> is significantly larger than between the proposed experimental counterparts and the assignments of 6<sup>+</sup>, 7<sup>+</sup>, and 8<sup>+</sup> spins to the 1787.3-, 1926.5-, and 2121.2-keV levels, respectively, is not final. In the experiment the three levels could have also spins 5<sup>+</sup>, 6<sup>+</sup>, and 7<sup>+</sup>, respectively, but in the semiempirical scheme described above there is no possibility to calculate a 5<sup>+</sup> level in <sup>88</sup>Br.

### C. Shell-model calculations for <sup>88</sup>Br

To verify the proposed picture, we have calculated excitations in <sup>88</sup>Br using the contemporary shell model in a large valence space including the  $(1f_{5/2}, 2p_{3/2}, 2p_{1/2}, 1g_{9/2})$  orbitals for protons and the  $(2d_{5/2}, 3s_{1/2}, 1g_{7/2}, 2d_{3/2}, 1h_{11/2})$  orbitals for neutrons, outside the <sup>78</sup>Ni core. Similar calculations have been performed in recent studies of even- $Z$ ,  $N = 52$  and  $N = 53$  isotones [3,5]. The effective interaction used in this work is based on the interaction described in Refs. [4,6], however, we have updated the proton-proton part of the interaction to reproduce the available data in  $N = 50$  isotones. In particular, new estimates for proton single-particle energies in the nickel core have been employed, resulting from our recent studies of exotic copper isotopes [40]. The calculations have been performed using the  $m$ -scheme shell model code ANTOINE [41] and in several cases the coupled-scheme code NATHAN [42]. The size of matrices in the considered valence space are of the order  $7 \times 10^6$  in the  $m$  scheme, thus full space diagonalizations are feasible. This is an important advantage of the <sup>78</sup>Ni core when studying exotic nuclei located above it. Therefore, further development of interactions in the proposed valence space and probing experimentally the single-particle structures in the vicinity of <sup>78</sup>Ni is particularly interesting for future shell-model applications.

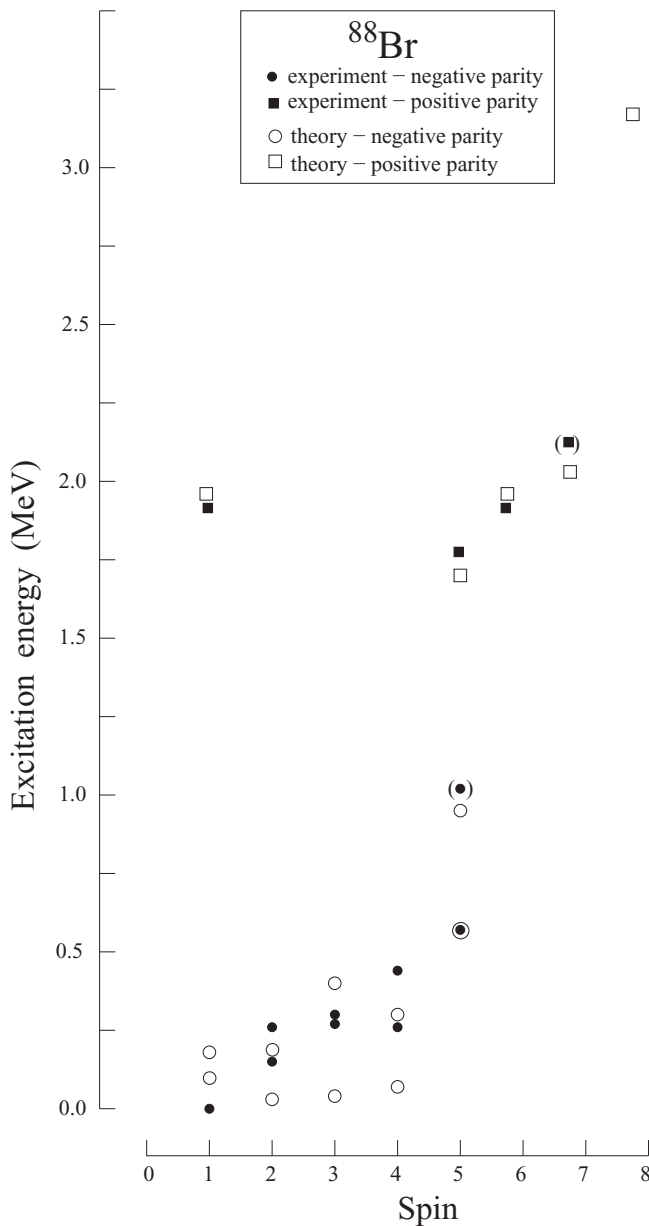


FIG. 12. Comparison of excited levels in  $^{88}\text{Br}$ , observed in this work, to the present shell-model calculations. Calculations are normalized to the experiment at the  $5_1^-$  level. The experimental  $1^+$  level is taken from Ref. [18].

In Fig. 12 the results of the calculations are compared to experimental levels in  $^{88}\text{Br}$  (the calculations are normalized, arbitrarily, to the experiment at the  $5_1^-$  level). The shell model reproduces well the overall scale of excitations in  $^{88}\text{Br}$ . The  $\pi p_{3/2} \nu d_{5/2}$  and the  $\pi f_{5/2}^{-1} \nu d_{5/2}$  multiplets, comprising negative-parity excitations with spins from  $1^-$  to  $5^-$  are calculated in the energy range from 0 to 0.6 MeV and the positive-parity levels are calculated above 1.7 MeV.

Within the  $\pi p_{3/2} \nu d_{5/2}$  and the  $\pi f_{5/2}^{-1} \nu d_{5/2}$  multiplets the experimental levels are reproduced satisfactorily, with deviations up to 200 keV for some levels, which is an average accuracy of the present shell-model calculations in this region.

TABLE V. Occupation of neutron and proton orbitals; calculated in this work for levels in  $^{88}\text{Br}$ , using the shell model. Particularly interesting numbers are shown in bold.

Levels	Neutrons					Protons			
	$d_{5/2}$	$s_{1/2}$	$g_{7/2}$	$d_{3/2}$	$h_{11/2}$	$f_{5/2}$	$p_{3/2}$	$p_{1/2}$	$g_{9/2}$
$1_1^-$	2.57	0.18	0.05	0.13	0.07	<b>4.41</b>	<b>1.95</b>	0.42	0.22
$2_1^-$	2.60	0.16	0.05	0.13	0.06	<b>4.53</b>	<b>1.86</b>	0.39	0.22
$3_1^-$	2.52	0.23	0.05	0.14	0.07	3.70	2.72	0.37	0.21
$4_1^-$	2.59	0.15	0.05	0.14	0.07	<b>4.63</b>	<b>1.80</b>	0.35	0.22
$4_2^-$	2.58	0.17	0.06	0.12	0.07	3.85	2.60	0.33	0.22
$5_1^-$	2.61	0.12	0.06	0.14	0.07	<b>4.46</b>	<b>1.94</b>	0.38	0.22
$5_2^-$	2.55	0.21	0.05	0.13	0.06	3.64	2.72	0.46	0.18
$6_1^-$	2.68	0.09	0.05	0.11	0.07	<b>4.25</b>	<b>2.25</b>	0.30	0.20
$1_1^+$	2.45	0.18	0.06	0.22	0.09	3.81	1.70	0.42	<b>1.07</b>
$5_1^+$	2.31	0.35	0.05	0.22	0.07	3.77	1.76	0.38	<b>1.09</b>
$6_1^+$	2.50	0.20	0.06	0.17	0.07	3.83	1.73	0.35	<b>1.10</b>
$7_1^+$	2.44	0.19	0.07	0.21	0.09	3.85	1.72	0.33	<b>1.10</b>
$8_1^+$	2.28	0.34	0.06	0.21	0.11	3.77	1.83	0.37	<b>1.03</b>
$9_1^+$	2.42	0.21	0.07	0.20	0.10	3.82	1.79	0.32	<b>1.07</b>

In Table V we show occupation of neutron and proton orbitals, calculated in this work for levels in  $^{88}\text{Br}$ . The shell model supports the  $\pi f_{5/2}^{-1} \nu d_{5/2}$  interpretation for the  $5_1^-$  and  $2_1^-$  levels and for the and  $4^-$  isomer proposed with the semiempirical picture, though also the ground state is assigned by the shell model to this multiplet, in contrast to the semiempirical picture here and in Ref. [19].

The  $5^+$ ,  $6^+$ , and  $7^+$  experimental candidates above 1.7 MeV, are reproduced very well when the 1787.3-keV level is assigned spin  $5^+$ . In the case where the 1787.3-keV level is assigned spin  $6^+$  and the 2121.2-keV level is assigned spin  $8^+$ , there is large discrepancy between the calculations and the experiment at spin  $8^+$  and no experimental candidate for spin  $5^+$ . The  $5^+$ ,  $6^+$ , and  $7^+$  calculated levels, all have in their wave function one proton in the  $g_{9/2}$  orbital, as expected for the  $(\pi g_{9/2}, \nu d_{5/2})$  dominating configuration (see Table V). We stress here that the shell model supports the presence of a multiplet of states connected with the  $(d_{5/2}^3)$ , seniority-3 configuration, coupled to the  $\pi g_{9/2}$  orbital.

The first  $8^+$  level, calculated at 2927 keV, does not have any obvious counterpart in the experiment (possible candidates are at 2613.0 and 3019.2 keV). It contains very little of the  $g_{7/2}$  neutron in its wave function, in contrast to semiempirical expectations. Analogous calculations for  $^{92}\text{Rb}$  predict an  $8^+$  level with one neutron in  $g_{7/2}$ , in good agreement with the experiment (see Table II in Ref. [9]). However, in  $^{92}\text{Rb}$ , which has five valence neutrons, the  $(\pi g_{9/2}, \nu g_{7/2})_{8^+}$  level is expected at lower energy than in  $^{88}\text{Br}$ . In  $^{88}\text{Br}$  the  $8^+$  level is probably due to the  $(\nu d_{5/2}^3)_{7/2^+}$  coupling, which requires extra energy for breaking the  $\nu d_{5/2}^2$  pair.

The  $(\pi g_{9/2}, \nu g_{7/2})_j$  particle-particle coupling should also produce a  $1^+$  level low in the multiplet. The  $1^+$  level at 1903.7 keV in  $^{88}\text{Br}$ , strongly populated in  $\beta$  decay of  $^{88}\text{Se}$  [18,25], might be a suitable candidate. The calculated level fits well the experiment and there is one proton in the  $\pi g_{9/2}$  orbital, but

again there is very little of  $g_{7/2}$  neutron in the wave function of this state.

Summarizing, the role of the  $g_{7/2}$  neutron orbital at  $N = 53$  seems to be insignificant. For example the  $6_1^-$  and  $8_1^+$  levels are calculated with very little of  $\nu g_{7/2}$ . However, the shell model clearly supports the  $(d_{5/2}^3)_{j,j-1}$ , anomalous coupling in  $^{88}\text{Br}$ . Furthermore, wave functions of the low-lying, negative-parity levels are quite similar, which suggests the presence of collective effects in  $^{88}\text{Br}$ , causing large configuration mixing within the  $\pi p_{3/2}\nu d_{5/2}$  and  $\pi f_{5/2}^{-1}\nu d_{5/2}$  multiplets.

#### D. Shell-model calculations for $^{86}\text{Br}$

To get further insight into the coupling of seniority-3,  $\nu d_{3/2}$  configuration with the  $\pi g_{9/2}$  orbital, we have performed shell-model calculations for  $^{86}\text{Br}$ , which has only one valence neutron. The same effective interaction as in  $^{88}\text{Br}$  have been used. Figure 13 compares the calculated to the experimental levels, reported in Ref. [27]. The calculations are normalized to the experiment at the  $5_1^-$  level.

The calculations reproduce well the overall scale of excitations in  $^{86}\text{Br}$ . The  $1^-$  to  $5^-$  members of the  $\pi p_{3/2}\nu d_{5/2}$  and the  $\pi f_{5/2}^{-1}\nu d_{5/2}$  multiplets are calculated in the energy range from 0 to 0.6 MeV and the positive-parity levels are calculated above 1.5 MeV, in agreement with the experiment [27].

The  $7^+$  level at 1.6 MeV is reproduced very well with one proton in the  $g_{9/2}$  orbital, as expected. However, for the  $6^+$  level in  $^{86}\text{Br}$  the picture is clearly different than in  $^{88}\text{Br}$ . The shell model predicts the first  $6^+$  excitation nearly 1 MeV above the  $7^+$  level. Such high energy may explain the nonobservation of the  $6^+$  level in Ref. [27]. This result supports our proposition of the  $6^+$  level in  $^{88}\text{Br}$  as the anomalous coupling of the three neutrons in the  $d_{5/2}$  orbital. Such a coupling is obviously not present in  $^{86}\text{Br}$ .

The model also reproduces well the position of the  $1^+$  experimental level [18,25] but the  $8_1^+$  level is calculated at very high energy of 3.5 MeV. Again both calculated levels do not have any  $g_{7/2}$  neutron in their wave functions. The high energy calculated for the  $8_1^+$  level may reflect both the high energy of the  $\nu g_{7/2}$  orbital in  $^{86}\text{Br}$  and the fact that the  $(\nu d_{5/2}^3)_{7/2^+}$  coupling is not available in  $^{86}\text{Br}$ . Still, there is a possible experimental  $8_1^+$  level at 2.7 or 3.2 MeV [27]. If confirmed, this would require an readjustment of the position of the  $\nu g_{7/2}$  single-particle energy in the  $^{78}\text{Ni}$  core and its evolution with the increasing proton number.

At the end, we note that in both  $^{86}\text{Br}$  and  $^{88}\text{Br}$  the second  $5^-$  level is predicted at a rather low energy of about 1 MeV. As discussed in Ref. [27] the first  $5^-$  level in  $^{86}\text{Br}$  is interpreted as the highest spin member of the  $(\pi f_{5/2}^{-1}\nu d_{5/2})$  multiplet and one expects only one such level. It is then interesting to ask what is the structure of the second  $5^-$  level. The present shell model gives the second  $5^-$  excited state dominated by  $(p_{3/2}^3)$  proton configuration coupled to the odd neutron in the  $d_{5/2}$  orbital in both bromine isotopes. Another possibility would be the promotion of the odd neutron to create the  $(\pi f_{5/2}^{-1}\nu g_{7/2})$  configuration, which may couple to spins from  $1^-$  to  $6^-$ . In  $^{88}\text{Br}$  there is a candidate for the  $5_2^-$  level at 1013.7 keV, close to the calculated  $5_2^-$  level. There are also possible experimental

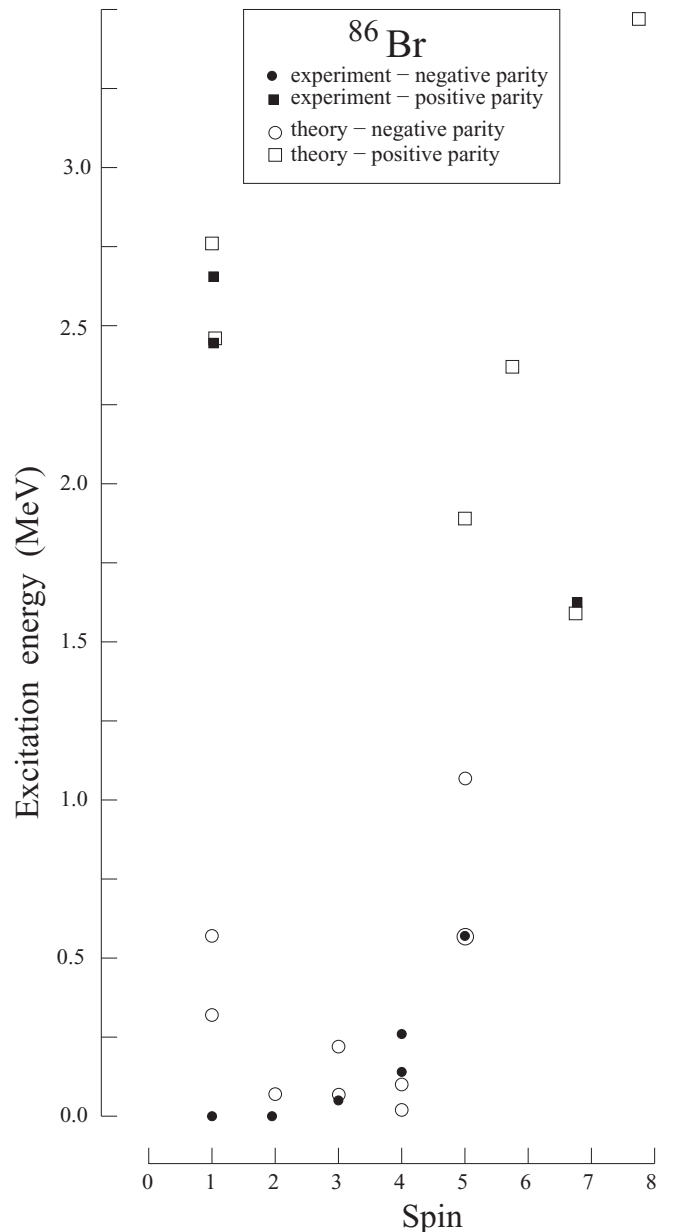


FIG. 13. Comparison of excited levels in  $^{86}\text{Br}$  [27] to the shell-model calculations performed in the present work. Calculations are normalized to the experiment at the  $5_1^-$  level. The experimental  $1^+$  level is taken from Ref. [18].

candidates for  $6^-$  excitations below 1.7 MeV in both nuclei. It is of interest to search for the second  $5^-$  level in  $^{86}\text{Br}$ . Studies of these levels may help verify the position of the intriguing  $g_{7/2}$  neutron level. We should note, however, that the  $6_2^-$  level in  $^{88}\text{Br}$  is calculated with little of  $\nu g_{7/2}$ , despite a simple semiempirical expectation that spin 6 could not be produced without this orbital.

#### IV. SUMMARY AND CONCLUSIONS

In summary, we have observed for the first time medium-spin yrast excitations in the odd-odd  $^{88}\text{Br}$  nucleus. The low-



energy, newly observed levels are identified as members of the  $\pi p_{3/2} \nu(d_{5/2})^3$  and  $\pi f_{5/2}^{-1} \nu(d_{5/2})^3$  multiplets, similar to those observed in  $^{86}\text{Br}$ . In the present work we support spin and parity  $1^-$  for the ground state of  $^{88}\text{Br}$ , proposed in Ref. [19], changing thus the ( $2^-$ ) assignment, adopted in the compilation [25].

Around 2 MeV of excitation a triplet of yrast levels is observed, interpreted as due coupling of the  $g_{9/2}$  proton to the  $(\nu d_{5/2})^3$ , seniority-3 multiplet, seen systematically in the odd- $A$ ,  $N = 53$  isotones. This observation supports the presence of collective effects proposed in our previous works [3,5]. Excitation energies of these states support the position of the  $g_{9/2}$  proton intruder in the  $^{78}\text{Ni}$  core at 5.7 MeV above the  $f_{5/2}$  proton level.

The Shell-model calculations agree very well with the experiment, when assigning spin  $5^+$  to the 1787.3-keV level in

$^{88}\text{Br}$ . It is of high importance to uniquely determine in further experiments spin and parity of this level. We also point to the need of further experimental work to uniquely identify in  $^{86}\text{Br}$  and  $^{88}\text{Br}$  the  $5_2^-$ ,  $6_1^-$ , and  $8_1^+$  levels. This should help determine the position of the neutron  $g_{7/2}$  orbital in Br isotopes, for which there are some ambiguities.

## ACKNOWLEDGMENTS

This work was supported by the Polish National Science Centre under Contract No. DEC-2013/09/B/ST2/03485 and by the Hungarian Scientific Research Fund, OTKA (Contracts No. K100835 and No. K106035). The authors thank the technical services of the ILL, LPSC, and GANIL for supporting the EXILL campaign. The Exogam Collaboration and the INFN Legnaro are acknowledged for the loan of Ge detectors.

- 
- [1] F.-K. Thielemann and K.-L. Kratz, in *Proceedings of the XXII Mazurian Lakes Summer School*, Poland, 1991 (IOP, Bristol, 1991), pp. 187–226.
- [2] W. Urban, T. Rząca-Urban, J. L. Durell, A. G. Smith, and I. Ahmad, *Eur. Phys. J A* **24**, 161 (2005).
- [3] T. Rząca-Urban, M. Czerwiński, W. Urban, A. G. Smith, I. Ahmad, F. Nowacki, and K. Sieja, *Phys. Rev. C* **88**, 034302 (2013).
- [4] K. Sieja, F. Nowacki, K. Langanke, and G. Martínez-Pinedo, *Phys. Rev. C* **79**, 064310 (2009).
- [5] M. Czerwiński, T. Rząca-Urban, K. Sieja, H. Sliwinska, W. Urban, A. G. Smith, J. F. Smith, G. S. Simpson, I. Ahmad, J. P. Greene, and T. Materna, *Phys. Rev. C* **88**, 044314 (2013).
- [6] K. Sieja, T. R. Rodriguez, K. Kolos, and D. Verney, *Phys. Rev. C* **88**, 034327 (2013).
- [7] A. Korgul, K. P. Rykaczewski, R. Grzywacz, H. Śliwińska, J. C. Batchelder, C. Bingham, I. N. Borzov, N. Brewer *et al.*, *Phys. Rev. C* **88**, 044330 (2013).
- [8] G. S. Simpson, W. Urban, K. Sieja, J. A. Dare, J. Jolie, A. Linneman, R. Orlandi, A. Scherillo, A. G. Smith, T. Soldner, I. Tsekhanovich, B. J. Varley, A. Złomaniec, J. L. Durell, J. F. Smith, T. Rząca-Urban, H. Faust, I. Ahmad, and J. P. Greene, *Phys. Rev. C* **82**, 024302 (2010).
- [9] W. Urban, K. Sieja, G. S. Simpson, T. Soldner, T. Rząca-Urban, A. Złomaniec, I. Tsekhanovich, J. A. Dare, A. G. Smith, J. L. Durell, J. F. Smith, R. Orlandi, A. Scherillo, I. Ahmad, J. P. Greene, J. Jolie, and A. Linneman, *Phys. Rev. C* **85**, 014329 (2012).
- [10] T. Rząca-Urban, K. Sieja, W. Urban, F. Nowacki, J. L. Durell, A. G. Smith, and I. Ahmad, *Phys. Rev. C* **79**, 024319 (2009).
- [11] A. Blanc *et al.*, in *Fifth International Workshop Nuclear Fission and Fission Product Spectroscopy 2013*, Caen, France [*EPJ Web Conf.* **62**, 01001 (2013)]; *J. Instrum.* (to be published).
- [12] H. Abele, D. Dubbers, H. Häse, M. Klein, A. Knöpfler *et al.*, *Nucl. Instrum. Methods A* **562**, 407 (2006).
- [13] J. Simpson, F. Azaiez, G. deFrance, J. Fouan, J. Gerl, R. Julin, W. Korten, P. J. Nolan, B. M. Nyakó *et al.*, *Acta Phys. Hung. New Ser.: Heavy Ion Phys.* **11**, 159 (2000).
- [14] D. Bazzacco *et al.*, in *Proceedings of the 5th International Seminar on Nuclear Physics*, edited by A. Covello (World Scientific, Singapore, 1999), pp. 417–430.
- [15] G. S. Simpson, J. C. Angeli, J. Genevey, J. A. Pinston *et al.*, *Phys. Rev. C* **76**, 041303(R) (2007).
- [16] W. Urban, M. Jentschel, B. Märkisch, Th. Materna, Ch. Bernards, C. Drescher, Ch. Fransen, J. Jolie, U. Köster, P. Mutti, T. Rząca-Urban, and G. S. Simpson, *J. Instrum.* **8**, P03014 (2013).
- [17] P. Mutti *et al.*, in *Proceedings of the Third International Conference on Advancements in Nuclear Instrumentation Measurement Methods and Their Applications (ANIMMA 2013)*, Marseille, France, June 23–27, 2013, edited by Dora Merelli (IEEE, New York, 2013).
- [18] M. Zendel, N. Trautmann, and G. Herrmann, *J. Inorg. Nucl. Chem.* **42**, 1387 (1980).
- [19] J. Genevey, F. Ibrahim and J. A. Pinston, H. Faust, T. Friedrichs, M. Gross, and S. Oberstedt, *Phys. Rev. C* **59**, 82 (1999).
- [20] W. Urban, W. R. Phillips, J. L. Durell, M. A. Jones, M. Leddy, C. J. Pearson, A. G. Smith, B. J. Varley, I. Ahmad, L. R. Morss, M. Bentaleb, E. Lubkiewicz, and N. Schulz, *Phys. Rev. C* **54**, 945 (1996).
- [21] S. K. Basu, G. Mukherjee, and A. A. Sonzogni, *Nucl. Data Sheets* **111**, 2555 (2010).
- [22] N. Nica, *Nucl. Data Sheets* **111**, 525 (2010).
- [23] K. S. Krane, R. M. Steffen, and R. M. Wheeler, *At. Data Nucl. Data Tables* **11**, 351 (1973).
- [24] I. Ahmad and W. R. Phillips, *Rep. Prog. Phys.* **58**, 1415 (1995).
- [25] E. A. McCutchan and A. A. Sonzogni, *Nucl. Data Sheets* **115**, 135 (2014).
- [26] P. M. Endt *At. Data Nucl. Data Tables* **26**, 47 (1981).
- [27] M.-G. Porquet, A. Asteir, Ts. Venkova, I. Deloncle, F. Azaiez, A. Buta, D. Curien, O. Dorvaux, G. Duchene, B. J. P. Gall *et al.*, *Eur. Phys. J A* **40**, 131 (2009).
- [28] J. P. Schiffer and W. W. True, *Rev. Mod. Phys.* **48**, 191 (1976).
- [29] O. Sorlin and M.-G. Porquet, *Prog. Part. Nucl. Phys.* **61**, 602 (2008).
- [30] R. L. Bunting, W. L. Talbert, Jr., J. R. McConnell, and R. A. Meyer, *Phys. Rev. C* **13**, 1577 (1976).
- [31] S. P. Pandya, *Phys. Rev.* **103**, 956 (1956).

- [32] J. Blomqvist, P. Kelnheinz, and P. J. Daly, *Z. Phys. A* **312**, 27 (1983).
- [33] J. Jongman, J. C. S. Bacelar, A. Balanda, R. F. Noorman, Th. Steenbergen, W. Urban, M. J. A. de Voigt, J. Nyberg, G. Sletten, J. Dionisio, Ch. Vieu, J. M. Lagrange, and M. Pautrat, *Nucl. Phys. A* **581**, 165 (1995).
- [34] M. Wang, G. Audi, A. H. Wapstra, F. G. Kondev, M. MacCormick, X. Xu, and B. Pfeiffer, *Chin. Phys. C* **36**, 1603 (2012).
- [35] M.-G. Porquet, Ts. Venkova, A. Astier, I. Deloncle, A. Prévost, F. Azaiez, A. Buta, D. Curien, O. Dorvaux, G. Duchene, B. J. P. Gall *et al.*, *Eur. Phys. J A* **28**, 153 (2006).
- [36] A. Astier, M.-G. Porquet, Ts. Venkova, G. Duchêne, F. Azaiez, D. Curien, I. Deloncle, O. Dorvaux, B. J. P. Gall, N. Redon, M. Rousseau, and O. Stézowski, *Phys. Rev. C* **88**, 024321 (2013).
- [37] S. Raman, B. Fogelberg, J. A. Harvey, R. L. Macklin, P. H. Stelson, A. Schröder, and K.-L. Kratz, *Phys. Rev. C* **28**, 602 (1983).
- [38] R. G. Helmer, *Nucl. Data Sheets* **95**, 543 (2002).
- [39] J. S. Thomas, G. Arbanas, D. W. Bardayan, J. C. Blackman, J. A. Cizewski, D. J. Dean, R. P. Fitzgerald, U. Griefe, C. J. Gross *et al.*, *Phys. Rev. C* **76**, 044302 (2007).
- [40] P. Morfouace *et al.* (unpublished); Zs. Vajta *et al.* (to be published).
- [41] E. Caurier and F. Nowacki, *Acta Phys. Pol. B* **30**, 705 (1999).
- [42] E. Caurier, G. Martinez-Pinedo, F. Nowacki, A. Poves, and A. P. Zuker, *Rev. Mod. Phys.* **77**, 427 (2005).